CHEMISTRY
A EUROPEAN JOURNAL

DOI: 10.1002/chem.200903420

Dispersion of HiPco® and CoMoCAT® Single-Walled Nanotubes (SWNTs) by Water Soluble Pyrene Derivatives—Depletion of Small Diameter SWNTs

Claudia Backes,[a, b] Udo Mundloch,[b] Alexander Ebel,[b] Frank Hauke,[a, b] and Andreas Hirsch*[a, b]

Despite the extraordinary electronic and mechanical properties of single-walled nanotubes (SWNTs), this most remarkable material has not yet entered the realm of industrial applications due to its polydispersity.[1] As-produced SWNTs contain a vast mixture of diameters and chiralities defining their electronic structure as being metallic or semiconducting.[2,3] Furthermore, the strong intertube van der Waals interactions of 500 $eV\,\mu m^{-1}$,[4] which render nanotubes virtually insoluble in common organic solvents and water, constrict any application. Among the efforts to increase the processability of this unique material, noncovalent functionalization of these systems represents a corner stone, as it is nondestructive; that is, it does not alter the intrinsic properties of nanotubes.[5–10] Furthermore, it has opened the door towards the development of efficient SWNT separation and sorting techniques.[11]

Most conveniently, SWNTs are dispersed in water with the aid of amphiphiles such as detergents.[12–15] In addition to the readily available detergents, bifunctional polycyclic aromatic compounds, such as perylene[16,17] and pyrene[18,19] derivatives, are also excellent candidates for the dispersion/dissolution of SWNTs. In principal, a strong and specific interaction with the SWNT can be ensured through π–π stacking, which is, in many cases, favorable over the nonspecific hydrophobic interaction exploited by classical detergents. The ideal scenario for nanotube solubilization would be the dispersion and selection of specific SWNTs in one step by the aid of a selectively individualizing surfactant. As this is a truly challenging task, any progress towards selective nanotube solubilization aiding the understanding of SWNT–surfactant interactions is bound to great impact.

Herein, we report on the solubilization of HiPco® and CoMoCAT® SWNTs by the water-soluble pyrene (pyr) derivatives **1** and **2**.[20] The dispersion and solubilization efficiency

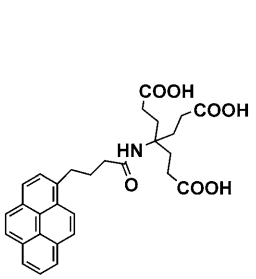

1

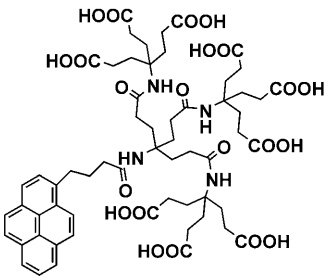

2

has been investigated by optical absorption and emission spectroscopy, as well as AFM, with comparison to the commercially available surfactant sodium dodecyl benzene sulfonate (SDBS). The supernatants of the CoMoCAT®–pyr dispersions are depleted from small diameter nanotubes pointing towards an increased interaction of the surfactants with larger diameter SWNTs.

In a typical dispersion experiment, the SWNT raw material (0.1 $g\,L^{-1}$) was immersed in the buffered aqueous solution of **1** or **2** (0.5 $g\,L^{-1}$, pH 7 or 10). After sonication (20 min), the homogeneous mixture was centrifuged (14 krpm, 30 min) in order to remove coarse aggregates and large SWNT bundles. The optical absorption spectra (pH 10, Figure 1 and pH 7 Figure S1 in the Supporting Information, respectively) of the supernatants reveal reasonably well-resolved excitonic nanotube transitions being indicative for well-dispersed SWNTs at low surfactant concentrations. The

[a] C. Backes, Dr. F. Hauke, Prof. Dr. A. Hirsch
Institute of Advanced Materials and Processes (ZMP)
University of Erlangen-Nuremberg
Dr. Mack Strasse 81, 90762 Fuerth (Germany)
Fax: (+49) 9131-85-26 864
E-mail: andreas.hirsch@chemie.uni-erlangen.de

[b] C. Backes, U. Mundloch, A. Ebel, Dr. F. Hauke, Prof. Dr. A. Hirsch
Department of Chemistry and Pharmacy
and Interdisciplinary Center of Molecular Materials (ICMM)
University of Erlangen-Nuremberg
Henkestrasse 42, 91054 Erlangen (Germany)

Supporting information for this article is available on the WWW under http://dx.doi.org/10.1002/chem.200903420.

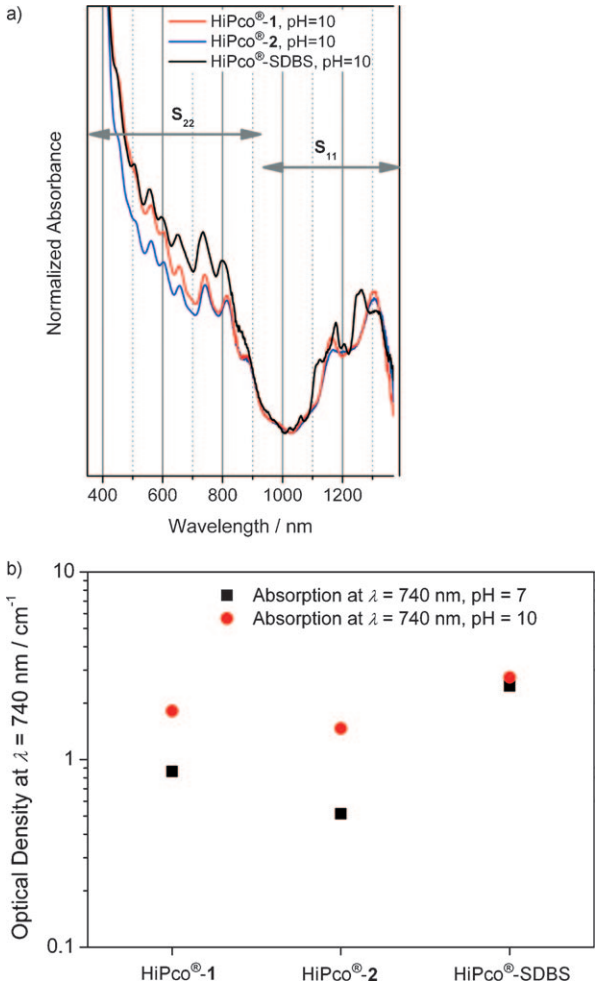

Figure 1. a) Optical absorption spectra normalized to the minimum of HiPco® SWNTs dispersed in buffered aqueous solutions of **1** and **2** (initial concentrations $[SWNT]_i = 0.1\,g\,L^{-1}$ and $[pyr]_i = 0.5\,g\,L^{-1}$, pH 10) compared to HiPco® SWNTs dispersed in SDBS (1 wt%, $[SWNT]_i = 0.1\,g\,L^{-1}$). The spectra of the supernatants after centrifugation are displayed. b) Optical density at $\lambda = 740$ nm of HiPco® SWNTs dispersed in aqueous solutions of **1**, **2**, and SDBS at pH 7 and 10.

nanotube concentration in the supernatant after centrifugation calculated from the extinction coefficients[17] and the optical density at 740 nm (Figure 1b) can be used as a measure for the dispersion efficiency of the surfactant.

As summarized in Table 1, the dispersion efficiency of the pyr surfactants is strongly enhanced at pH 10—an observation that can be attributed to an increased exfoliation during the sonication-induced unzippering of the nanotubes due to a higher charge density of the dendrimer head groups, as previously described for perylene derivatives equipped with Newkome-type dendrimers.[17]

Table 1. Tabulated calculated SWNT concentrations in the supernatant of SWNT–pyr after centrifugation with initial concentrations $[SWNT]_i = 0.1\,g\,L^{-1}$ and $[pyr]_i = 0.5\,g\,L^{-1}$. The concentration of SDBS is $10.0\,g\,L^{-1}$.

		1	**2**	SDBS
$[HiPco^®]$ $[g\,L^{-1}]$	pH 7	0.024	0.014	0.068
	pH 10	0.046	0.037	0.069

Significantly, the dispersion efficiency of **2** is reduced compared to **1** even though **2** is characterized by a higher intrinsic solubility due to the nine carboxylic acid functionalities opposed to the three such groups in **1**. Presumably, **2** can be less densely packed and organized on the nanotube scaffold due to the higher inter-pyrene coulombic repulsion between adjacent pyrene head groups, resulting in a reduced SWNT dispersion efficiency.

The dispersions were furthermore subjected to fluorescence spectroscopy. In general, the nanotube emission intensity is strongly reduced compared to nanotubes dispersed in aqueous solutions of SDBS. After diluting the samples to the same optical density, the SWNT emission appeared to be independent of the pyrene derivative and the pH (Figure S2 in the Supporting Information) strongly indicating that the nanotube emission pattern is dependent on the adsorption of the pyrene unit alone without contributions from the substituents or the pH medium. Upon comparing the nanotube emission pattern of the pyrene dispersions with the dispersion in SDBS, a pronounced red-shift of the spectral features is discernable. In contrast to the previously investigated perylene derivatives,[16] this red-shift is more pronounced for larger diameter nanotubes (Figure 2) compared to the smaller diameter nanotubes.

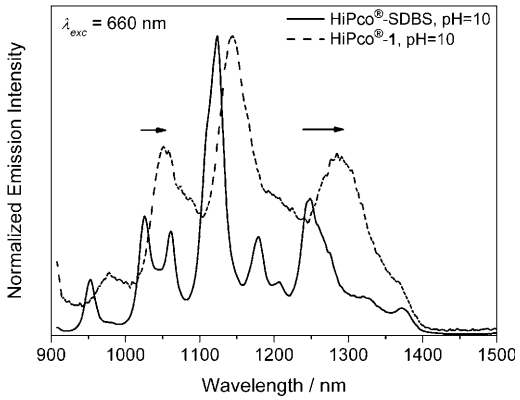

Figure 2. NIR emission spectra normalized to the emission maximum of HiPco® SWNTs dispersed in aqueous solutions of **1** and SDBS ($[SWNT] = 0.046\,g\,L^{-1}$ and $[\mathbf{1}]_i = 0.5\,g\,L^{-1}$, $[SDBS] = 10\,g\,L^{-1}$) at $\lambda_{exc} = 660$ nm after degassing with nitrogen prior to the acquisition of the spectra.

This observation may be rationalized by the hypothesis that the SWNT–pyr interaction is stronger for larger diameter nanotubes, as an enhanced interaction may lead to an increased alteration of the exciton binding energy. This is in marked contrast to the adsorption affinity of the perylene derivatives, which exhibit a more pronounced interaction with smaller diameter SWNTs. To further probe this impression, we have expanded the diameter range of the SWNTs in the region of small diameters by using CoMoCAT® SWNTs, which are characterized by a smaller and narrower

diameter distribution (0.7–0.9 nm) compared to the HiPco® material (0.8–1.4 nm). That is, the average diameter is smaller by 30% in the CoMoCAT® SWNTs.

For the set of experiments described in the following we have focused on the derivative **1** at pH 10, as it yields the highest dispersion efficiency. After dispersing CoMoCAT® SWNTs (0.1 g L^{-1}) in **1** (0.5 g L^{-1}), we found that the concentration of SWNTs in the supernatant after centrifugation with identical parameters was 0.037 g L^{-1}; that is, 22% lower compared to the HiPco® material (calculated from the optical density of 0.41 cm^{-1} at 652 nm and the extinction coefficient of CoMoCAT® SWNTs determined to be 1125 L g^{-1} m^{-1}). Furthermore, no transitions of very small diameter nanotubes in the region of 800–930 nm ((6,4)- and (9,1)-SWNTs) are discernable in CoMoCAT®–**1** (Figure 3a). However, such an indicated depletion may also be attributed to changes in the dielectric environment of the nanotube due to the adsorption of the pyrene derivatives. To ensure comparability with the pristine material dispersed in SDBS, **1** was replaced by the addition of SDBS to the CoMoCAT®–**1** sample. Such a replacement can be mapped by fluorescence spectroscopy, as the original nanotube emission pattern is obtained after removal of the pyrene surfactant from the nanotube sidewall (Figure S3 in the Supporting Information). The transitions of the (6,4) and (9,1)-nanotubes are not recovered after the addition of SDBS, indicative for depletion of the very small diameter nanotubes in the pyrene dispersed supernatant (Figure 3b). Both features are clearly present in the SDBS redispersed precipitate of CoMoCAT®–**1**.

In line with the absorption spectra, the fluorescence spectra at 580 nm excitation (Figure 4) also point towards an increased interaction of **1** with larger diameter nanotubes leading to insufficient solubilization of the (6,4)-SWNT and thus loss of the (6,4)-SWNT emission.

Additional evidence can be obtained from the individualization degrees determined from statistical atomic force microscopic (AFM) analysis of the CoMoCAT®–**1** and HiPco®–**1** supernatants spin-casted on silicon wafers. In all cases, AFM images were recorded until the height of at least 250 SWNT objects could be determined. Figure 5 depicts the histograms of the bundle size distributions of SWNT–**1**. Most importantly, the relative abundance of individual nanotubes is between 20–25% underlining the surfactant capability of the designed pyrene surfactants. We would like to point out that the individualization degree for the HiPco®–**1** sample is higher with respect to the CoMoCAT®–**1** dispersion, again pointing towards a more pronounced dispersion of larger diameter nanotubes by the pyrene surfactant.

In summary, we have demonstrated the surfactant capability of pyrene-based amphiphiles equipped with Newkome-type dendrimers. The dispersion efficiency is highest for the first-generation Newkome dendronized pyrene **1** in basic media (pH 10). A more detailed investigation has pointed towards the preferential solubilization of larger diameter nanotubes; for example, a depletion of small diameter nanotubes in the CoMoCAT®–**1** supernatant after mild centrifugation is observed, in marked contrast to anionic perylene-based surfactants that show enhanced adsorption towards smaller diameter SWNTs. Even though the selectivity in the disperseability is not very pronounced, the observations may lead to a more detailed understanding of the interactions of SWNTs with π surfactants. A fine tuning of the indicated selectivity may be possible by variation of the substituents

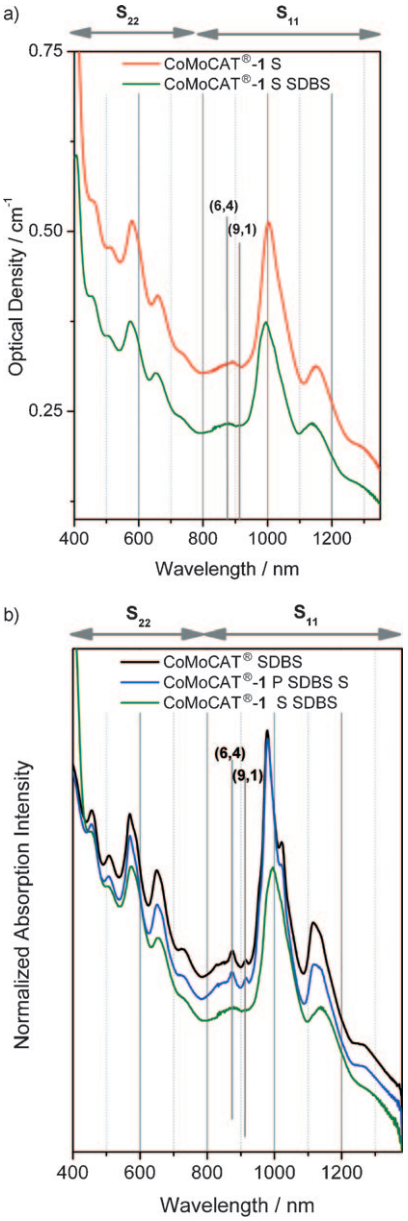

Figure 3. a) As recorded optical absorption spectrum of the supernatant after centrifugation (S) of CoMoCAT® dispersed in a buffered aqueous solution of **1** compared to the same dispersion after addition of an aqueous solution of SDBS (0.25 mL, 10 g L^{-1}) to CoMoCAT®–**1** (0.75 mL). b) UV/Vis/NIR absorption spectra normalized to the minimum of CoMoCAT® dispersed in SDBS ([SDBS] = 10 g L^{-1}) and the SDBS redispersed supernatant and precipitate (P) after predispersion with **1** for comparison—vertical offset for clarity. ([SWNT] = 0.027 g L^{-1}, $[\mathbf{1}]_i$ = 0.5 g L^{-1}, pH 10).

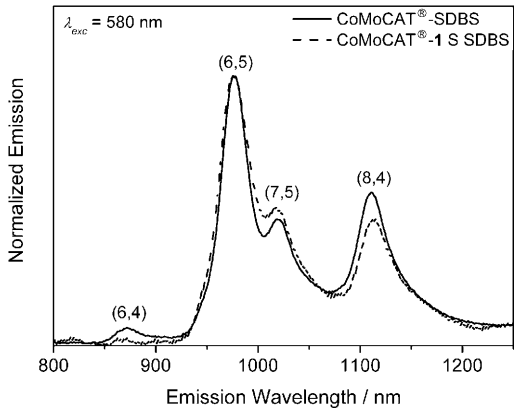

Figure 4. Normalized emission spectra with $\lambda_{exc}=580$ nm of CoMoCAT®-SDBS and the supernatant (S) of CoMoCAT®–**1** after replacement of **1** with SDBS; an aqueous solution of SDBS (0.25 mL, 10 g L^{-1}) was added to CoMoCAT®–**1** (0.75 mL) with [**1**]$_i$ = 0.5 g L^{-1}). The dispersions were diluted prior to acquisition of the spectra to an optical density of 0.37 cm^{-1} at 580 nm corresponding to a nanotube concentration of 0.027 g L^{-1}.

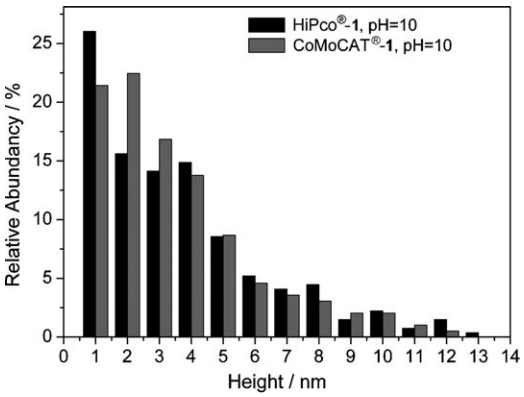

Figure 5. Histograms of the bundle size distributions of HiPco® and CoMoCAT® nanotubes dispersed in a buffered aqueous solution of **1** ([HiPco®] = 0.046 g L^{-1}, [CoMoCAT®] = 0.037 g L^{-1} [**1**] = 0.5 g L^{-1}) derived from statistical AFM analysis after spin-casting the supernatants.

and/or optimization of the surfactant to nanotube ratio. Further investigations towards reaching the goal of SWNT separation by selective dispersion on the basis of π surfactants are currently on the way in our laboratory.

Acknowledgements

We thank the Deutsche Forschungsgemeinschaft (DFG), the Interdisciplinary Center for Molecular Materials (ICMM), the Excellence Cluster Engineering of Advanced Materials (EAM) and the Graduate School Molecular Science (GSMS) for financial support.

Keywords: nanotubes · noncovalent functionalization · polycycles · selectivity · surfactants

[1] D. Tasis, N. Tagmatarchis, A. Bianco, M. Prato, *Chem. Rev.* **2006**, *106*, 1105.
[2] R. C. Haddon, J. Sippel, A. G. Rinzler, F. Papadimitrakopoulos, *MRS Bull.* **2004**, *29*, 252.
[3] D. Tasis, N. Tagmatarchis, V. Georgakilas, M. Prato, *Chem. Eur. J.* **2003**, *9*, 4000.
[4] L. A. Girifalco, M. Hodak, R. S. Lee, *Phys. Rev. B* **2000**, *62*, 13104.
[5] P. C. Ke, *Phys. Chem. Chem. Phys.* **2007**, *9*, 439.
[6] L. Vaisman, H. D. Wagner, G. Marom, *Adv. Colloid Interface Sci.* **2006**, *128–130*, 37.
[7] J. N. Coleman, *Adv. Funct. Mater.* **2009**, *19*, 3680.
[8] P. Singh, S. Campidelli, S. Giordani, D. Bonifazi, A. Bianco, M. Prato, *Chem. Soc. Rev.* **2009**, *38*, 2214.
[9] Y.-L. Zhao, J. F. Stoddart, *Acc. Chem. Res.* **2009**, *42*, 1161.
[10] D. I. Schuster, J. D. Megiatto, Jr., *Nat. Chem.* **2009**, *1*, 182.
[11] M. C. Hersam, *Nat. Nanotechnol.* **2008**, *3*, 387.
[12] M. F. Islam, E. Rojas, D. M. Bergey, A. T. Johnson, A. G. Yodh, *Nano Lett.* **2003**, *3*, 269.
[13] W. Wenseleers, I. I. Vlasov, E. Goovaerts, E. D. Obraztsova, A. S. Lobach, A. Bouwen, *Adv. Funct. Mater.* **2004**, *14*, 1105.
[14] T. Okazaki, T. Saito, K. Matsuura, S. Ohshima, M. Yumura, S. Iijima, *Nano Lett.* **2005**, *5*, 2618.
[15] O. Matarredona, H. Rhoads, Z. Li, J. H. Harwell, L. Balzano, D. E. Resasco, *J. Phys. Chem. B* **2003**, *107*, 13357.
[16] C. Backes, C. D. Schmidt, F. Hauke, C. Boettcher, A. Hirsch, *J. Am. Chem. Soc.* **2009**, *131*, 2172.
[17] C. Backes, C. D. Schmidt, K. Rosenlehner, J. N. Coleman, F. Hauke, A. Hirsch, *Adv. Mater.* **2009**, *22*, 788.
[18] T. Fujigaya, N. Nakashima, *Polym. J.* **2008**, *40*, 577.
[19] V. Sgobba, A. Troeger, R. Cagnoli, A. Mateo-Alonso, M. Prato, F. Parenti, A. Mucci, L. Schenetti, D. M. Guldi, *J. Mater. Chem.* **2009**, *19*, 4319.
[20] A. Ebel, W. Donaubauer, F. Hampel, A. Hirsch, *Eur. J. Org. Chem.* **2007**, 3488.

Received: December 14, 2009
Published online: February 24, 2010

